NJC

Accepted Manuscript

This is an *Accepted Manuscript*, which has been through the Royal Society of Chemistry peer review process and has been accepted for publication.

Accepted Manuscripts are published online shortly after acceptance, before technical editing, formatting and proof reading. Using this free service, authors can make their results available to the community, in citable form, before we publish the edited article. We will replace this *Accepted Manuscript* with the edited and formatted *Advance Article* as soon as it is available.

You can find more information about *Accepted Manuscripts* in the Information for Authors.

Please note that technical editing may introduce minor changes to the text and/or graphics, which may alter content. The journal's standard Terms & Conditions and the Ethical guidelines still apply. In no event shall the Royal Society of Chemistry be held responsible for any errors or omissions in this *Accepted Manuscript* or any consequences arising from the use of any information it contains.

ROYAL SOCIETY OF CHEMISTRY

www.rsc.org/njc

Facile synthesis of ZnO/C nanocomposites with enhanced photocatalytic activity

Jinjuan Xue‡, Shuaishuai Ma‡,Yuming Zhou,* Zewu Zhang

School of Chemistry and Chemical Engineering, Southeast University, Nanjing 211189, P. R. China

Abstract This manuscript presents a facile route for the preparation of ZnO/C nanocomposites using zinc citrate dihydrate as precursor though one-step calcination under nitrogen atmosphere. The products were characterized by X-ray diffraction (XRD), energy-dispersive X-ray spectroscopy (EDS), transmission electron microscopy (TEM), raman spectroscopy and ultraviolet-visible diffuse reflectance spectroscopy (UV-vis DRS). The results demonstrated ZnO nanoparticles sized 5-10 nm were distributed on the carbonaceous layers to form the ZnO/C nanocomposites. The as-prepared ZnO/C nanocomposites exhibited enhanced photocatalytic activity compared to pure ZnO with respect to methylene blue (MB) degradation under UV irradiation, which was benefit from the improved separation of photogenerated electrons and holes with the presence of carbonaceous layers. In particular, the rate of degradation methylene blue (MB) with ZnO/C(550N) as the photocatalyst is 4.15 times faster than that of using bare ZnO nanoparticles. Furthermore, the ZnO/C nanocomposites could be easily recycled without obvious decrease of the photocatalytic activity. It is believed that the resultant ZnO/C nanocomposites have potential applications in photocatalysis and environmental protection.

1 Introduction

* Corresponding author. Tel.: +86 25 52090617; fax: +86 25 52090617.
E-mail address: ymzhou@seu.edu.cn (Yuming Zhou).
‡S.S. Ma and J.J. Xue contributed equally to this work.

The increasing environmental contamination from textile dyes and other industrial dyes tuffs is becoming an overwhelming problem all over the world. Photocatalysis is a promising technique for solving many current environmental and energy issues through its efficiency and broad applicability.[1] Among the most studied semiconductors (e.g., TiO_2, ZnO, SnO_2, etc.) for photocatalytic applications,[2-4] zinc oxide (ZnO) has grown considerably, due to its physical and chemical stability, high catalytic activity, low cost, environmental friendliness and easy of availability.[5, 6] However, the poor utilization of solar energy and the short diffusion length of a photogenerated electron-hole pair are the two major factors limiting the further improvement of photocatalytic efficiency.[7] Some effort has been devoted to reducing the recombination of photogenerated electron-hole pairs and improving the utilization of solar light of ZnO, such as doping,[8, 9] deposition of metals,[10, 11] combining ZnO with another semiconductor,[12-14] or hybridizing ZnO with carbon materials.[15-17] In particular, carbonaceous materials have been widely used as ideal electron pathways due to their good conductivity. Some results have demonstrated that carbon materials could efficiently capture and transport of photogenerated electrons because of their highly conductive activity.[7, 17-19] To date, several studies have been reported that the photocorrosion of the ZnO catalysts and the photocatalytic performance of ZnO in the UV light irradiation can be improved by hybridizing ZnO with carbon materials, for instance, ZnO-carbon nanofiber heteroarchitectures,[15] carbon-coated ZnO nanorods,[19] ZnO nanoparticles hybridized with graphite-like carbon,[20] ZnO hybridized with graphene[21] and ZnO hybridized with C_{60}.[22] Despite the great progress made thus far, how to fabricate ZnO-based photocatalysts with tuned structure and excellent photocatalytic activity and stability by a simple procedure remains a big challenge.

Herein, we demonstrate a successful attempt for the fabrication of ZnO/C composites via a simple calcination method with zinc citrate dihydrate as precursor. This protocol does not need expensive equipment, complex process control, and stringent reaction conditions, and thus is simple and cost-effective. The prepared samples were characterized by X-ray diffraction (XRD), energy-dispersive X-ray spectroscopy (EDS), transmission electron microscopy (TEM) and high resolution transmission electron microscopy (HRTEM), raman spectroscopy and ultraviolet-visible diffuse reflectance spectroscopy (UV-vis DRS). The results indicated that ZnO nanoparticles were distributed uniformly on the carbonaceous layers. By forming the ZnO/C nanocomposites, one might be able to take advantage of both components. As expected, the as-obtained product exhibits enhanced photocatalytic activity for the degradation of methylene blue (MB) under UV light compared with bare ZnO nanoparticles.

2 Experimental Section

2.1 Marerials

Zinc citrate dihydrate and methylene blue (MB) were purchased from Aladdin Chemical Regent Co., Ltd. (Shanghai, China). All the reagents in this experiment are analytically pure and used without further purification.

2.2 Synthesis of ZnO/C nanocomposites and bare ZnO nanoparticles

The precursor zinc citrate dihydrate (0.5 g) was placed into a quartz boat and heat-treated in a tube furnace at 550 ^{o}C under nitrogen atmosphere for 3 h with a heating rate of 10 ^{o}C/min. After calcination, the sample had changed its color from the initial white to black, suggesting the existence of carbon component in the product. The black-colored product was collected

and marked as ZnO/C(550N). For comparison, bare ZnO nanoparticles were prepared by the same method, except for that the calcination atmospheric condition changed to air atmosphere. The obtained sample was marked as ZnO(550A).

2.3 Characterization

X-ray diffraction (XRD) measurement was carried out using a SmartLab XRD spectrometer (Rigaku) with Cu Kα radiation in the range of 10-70° (2θ). Energy dispersive X-ray spectroscopy (EDS) was used to analyze the composition of samples. Transmission electron microscopy (TEM; JEM-1230) and high resolution TEM (HRTEM) were used to characterize the morphologies of the products. Raman spectroscopy was performed using a Renishaw micro-Raman spectroscopy. Ultraviolet-visible diffuse reflectance spectroscopy (UV-vis DRS) of the samples were recorded on a UV-vis spectrophotometer (UV-3600, Shimadzu) with an integrating sphere attachment. The nitrogen adsorption and desorption isotherms were measured at 77 K on an ASAP 2020 (Micromertics USA). PL spectra were measured using room temperature photoluminescence with a 325 nm He-Cd laser excitation wavelength (Shimadzu RF-5301).

2.4 Photocatalytic Activity

The photocatalytic decomposition of MB solution (10 mg/L) was chosen as a model reaction to evaluate the photocatalytic activity of the samples. 20 mg of the ZnO/C(550N) was dispersed in the MB solution (100 mL) in a cylindrical glass jacketed reactor equipped with reflux water to keep the reaction temperature constant. After stirring in the dark for 30 min to reach an adsorption-desorption equilibrium between the photocatalyst and MB dye, the suspension was exposed to UV irradiation (250 W, GY-250, λ=365nm) with stirring. During

the process of photodegradation, 3 mL of the suspension was sampled every five minutes and centrifuged to get clear liquid for UV-vis characterization (UV-3600; Shimadzu) to determine the contents of MB. Control experiment of degradation MB by using ZnO(550A) was also carried out under identical conditions.

3 Results and Discussion

3.1 Structure and Morphology

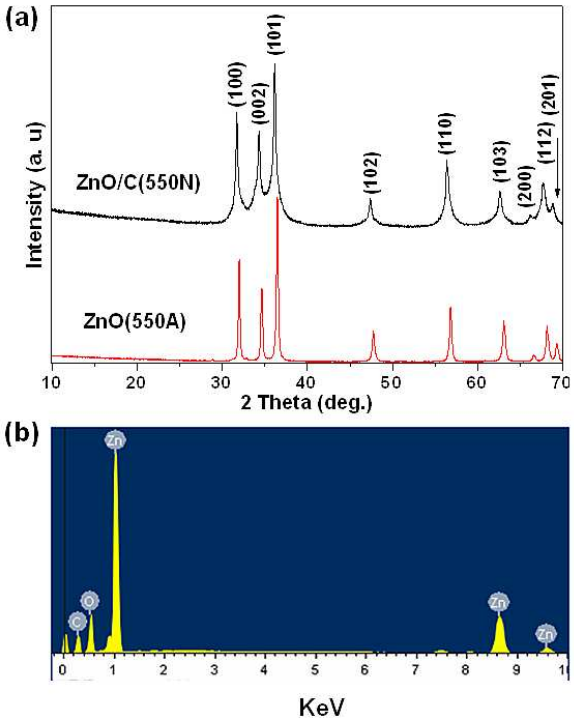

Fig. 1 XRD patterns of (a) ZnO(550A) and the as-prepared ZnO/C(550N) nanocomposites, and EDS spectrum of (b) the ZnO/C(550N).

The structure of ZnO/C(550N) nanocomposites was characterized by X-ray diffraction (XRD, Fig. 1 (a)), as a comparison, the XRD pattern of ZnO(550A) was also included. It can be found that all the diffraction peaks in the pattern of ZnO(550A) can be indexed a hexagonal phase of wurtzite-type ZnO with lattice constants a = 3.249 Å and c = 5.206 Å, in accordance with the standard data (JCPDS Card No. 65-3411). For comparison, all of the

diffraction peaks of ZnO/C(550N) nanocomposites also can be indexed to ZnO in a hexagonal structure; their strong and sharp features suggest that ZnO nanoparticles distributed on the carbonaceous layers were still well crystalline, like the ZnO(550A) sample. The difference between the XRD patterns of ZnO/C(550N) and ZnO(550A) is that the noise level of the former is higher, which is resulted from the scattering of X-rays caused by the amorphous carbon layers. The EDS pattern (Fig. 1 (b)) further demonstrated that the sample was only composed of Zn, O, and C atoms.

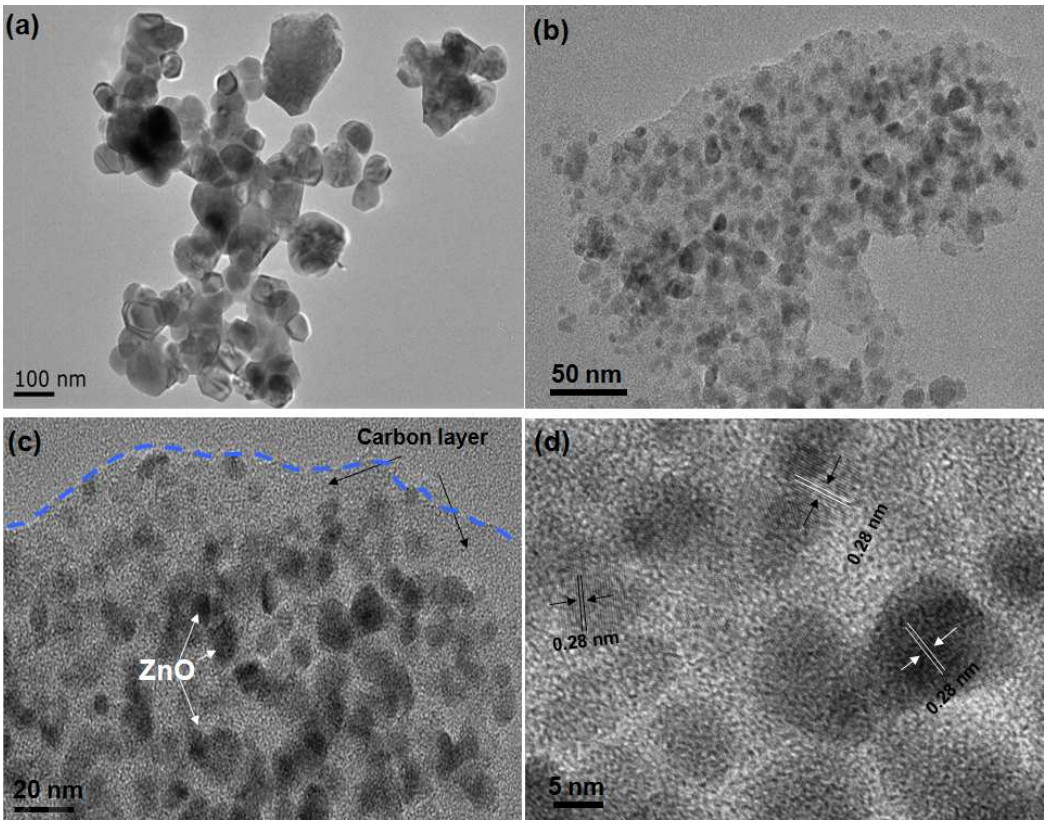

Fig. 2 Typical TEM images of (a) ZnO(550A) and (b and c) as-prepared ZnO/C nanocomposites, (d) HRTEM image of the as-prepared ZnO/C nanocomposites.

Transmission electron microscopy (TEM) and high resolution TEM (HRTEM) images are taken to directly analyze the morphology of the as-prepared samples, as displayed in Fig. 2. From Fig. 2 (a), it can be seen that ZnO(550A) nanoparticles normally ranges from 50 to

100 nm. As can be observed from Fig. 2 (b and c), the appeared obvious edge indicated that carbonaceous material existed in the composites was in the form of layers. And the ZnO nanoparticles sized 5-10 nm were densely deposited on the carbonaceous layers, implying that the ZnO nanoparticles and carbonaceous layers were integrated with an intimate interfacial contact by the current calcination approach. From the HRTEM image (in Fig. 2d), the lattice spacing of 0.28 nm corresponds to the inter-planar distance between adjacent (100) planes of the wurtzite ZnO. Moreover, the transparency of the carbon sheets also suggested that the as-prepared ZnO/C(550N) had a high porosity. Since the transfer process of photogenerated charge carriers in the RGO-semiconductor nanocomposites is intimately related to the interfacial interaction between RGO and the semiconductor,[23] it could be expected that such an intimate interfacial contact for the ZnO/C nanocomposites would favor the charge carrier transfer process, thus leading to the improvement of the photocatalytic performance.

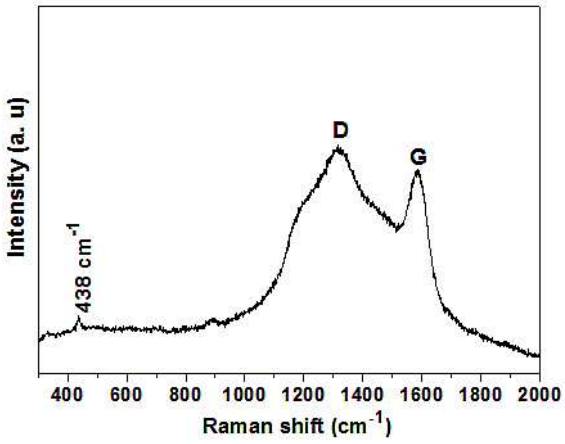

Fig. 3 Raman spectrum of the as-prepared ZnO/C nanocomposites.

The Raman spectrum of the as-prepared ZnO/C nanocomposites was recorded in the range of 300-2000 cm^{-1} as shown in Fig. 3. From Fig. 3, the small peak centered at about 438 cm^{-1} can be ascribe to high-frequency vibration modes of E_2, corresponding to a band

characteristic of wurtzite phase of ZnO.[24] Besides, another two peaks appeared at around 1590 and 1320 cm^{-1}, corresponding to the G- and D-bands, respectively, which are characteristic of typical carbon materials.[25] The G-band appearing around 1590 cm^{-1} is a significant characteristics of sp^2 hybridized carbon materials, which can provide information on the inplane vibration of sp^2-bonded carbon domains,[26, 27] whereas the D-band appears at around 1320 cm^{-1} indicate the presence of sp^3 defects within the hexagonal graphitic structure[28] and can be associated with the hexagonal graphitic structure and the amorphous carbon, or edges that break the symmetry and selection rule.[29, 30]

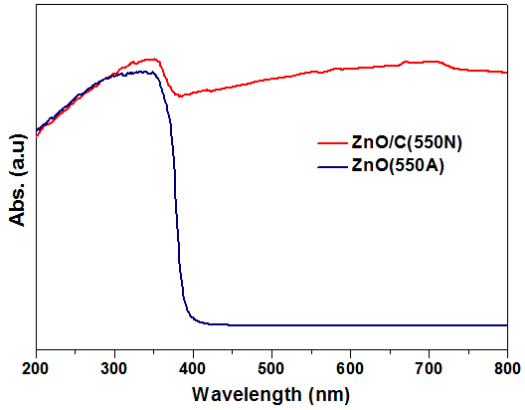

Fig. 4 UV-vis diffuse reflectance spectra of ZnO(550A) and ZnO/C(550N) nanocomposites.

The absorption range of light plays an important role in the photocatalysis. The optical absorption properties of ZnO(550A) and ZnO/C(550N) samples were measured with UV-vis diffuse reflectance spectroscopy (DRS) and the results are demonstrated in Fig. 4. It is noted that ZnO(550A) shows a steep adsorption edge located at 380 nm and an absorption band lower than 380 nm (UV region). Compared with ZnO(550A), ZnO/C(550N) displays strong capability of light absorption in both UV and visible light range of 200-800 nm. It is resulted from that the carbon layers incorporated in the nanocomposites modified the optical properties of ZnO with enlarging light absorption range, which is similar to carbon

nanotubes-ZnO and C-doped TiO_2 studies.[31, 32]

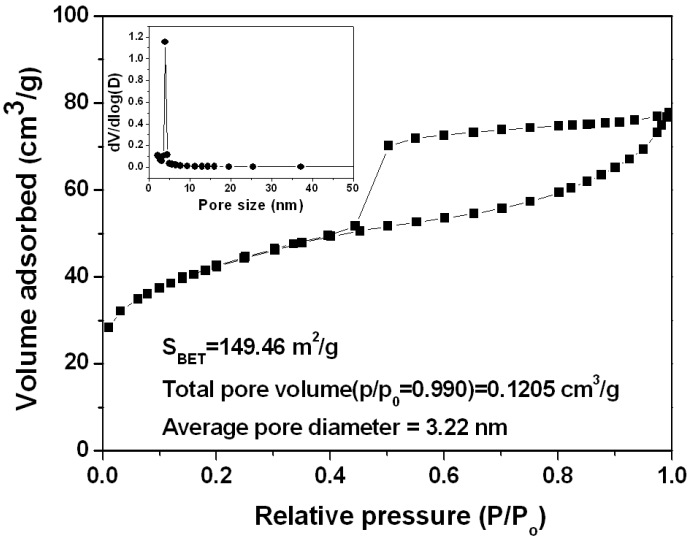

Fig. 5. N_2 adsorption-desorption isotherm and pore size distribution (inset) of the synthesized ZnO/C(550N) nanocomposites.

In Fig. 5, the N_2 adsorption-desorption isotherm, determined at various relative pressure (P/P_o) on the synthesized ZnO/C nanocomposites, exhibited type IV-like isotherms with H2 hysteresis loops according to IUPAC,[33] which are associated with capillary condensation taking place in mesopores. The pore size distribution curve (inset of Fig. 5) calculated from adsorption branch of the isotherms exhibited a maximum at 3.85 nm and the Brunauer-Emmett-Teller (BET) surface area of ZnO/C nanocomposites was calculated to be 149.46 m^2/g， which is much higher than that of ZnO(550A) (4.24 m^2/g).

3.2 Photocatalytic Activity

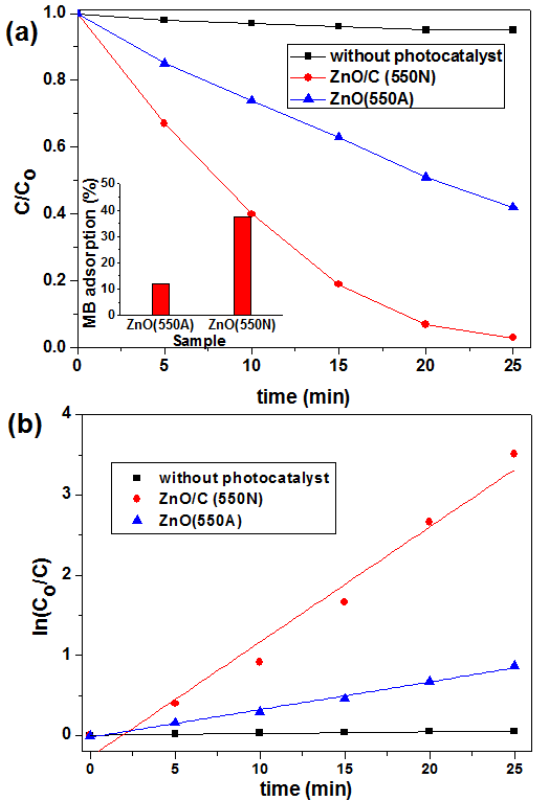

Fig. 6 Photocatalytic activities (a) and kinetics (b) of the as-prepared ZnO/C(550N) nanocomposites and ZnO/C(550A) for degradation of MB under UV light irradiation. Inset: adsorption capacities of ZnO/C(550N) and ZnO/C(550A).

Fig. 6 (a) inset shows the MB adsorption capacities of ZnO(550A) and ZnO/C(550N) samples. Adsorption-desorption equilibrium was reached within 30 min for most samples, as reported previously.[34, 35] As can be seen, the adsorption capacity of the ZnO/C(550N) sample (37.3%) is noticeably higher than that of ZnO(550A) (11.7%). The different adsorption capacity between the two samples is probably attributed to that the carbonaceous species existed in the ZnO/C(550N) sample is the main driving force for dye adsorption by the interactions between the graphitic carbon layer (sp^2 bonding) and the aromatic rings of the dye molecules. [36] Furthermore, the BET surface area of ZnO/C(550N) (147.20 m^2/g) is much higher than ZnO/C(550A) (4.24 m^2/g), which is also an important influential factor for adsorption capacity of the samples.[37]

The photocatalytic activities of the ZnO (550A) and ZnO/C (550N) were evaluated by measuring the decomposition of MB under UV irradiation. The change in absorption spectra of MB aqueous solution showed the change of its concentration. The initial concentration (C_o), the final concentration (C), and the degradation rate (D%) had a mathematical expression as follows:[38]

$$\text{MB decomposition } D\ (\%) = 100 \times (C_o - C) / C_o \qquad (1)$$

As observed in Fig. 6 (a), the concentration of MB has no significant change without catalyst under UV irradiation for 25 min. However, the MB degradation rate for ZnO/C(550N) nanocomposites can reach 99.7% in 25min under UV irradiation, while ZnO(550A) can only approach 58% for the same irradiation time. Obviously, the ZnO/C(550N) nanocomposites showed much higher photocatalytic activity than that of ZnO (550A), which is achieved as a result of the synergetic effects between the small ZnO nanoparticles and the carbonaceous layers. Furthermore, to quantitatively understand the reaction kinetics of MB degradation over different samples in our experiments, we re-plotted the data in Fig. 6 (b) according to the pseudo-first-order kinetic model as expressed by equation (2), which is generally used for photocatalytic degradation process take place at the interface between the catalysts and the organic pollutants with low concentration.[39]

$$\ln (C_o/C) = kt \qquad (2)$$

Where, t is reaction time, k is the rate constant, C_o and C are the concentrations of MB solution at time 0 and t, respectively. As can be seen, the psedudo-first-order rates constants for the photodegradation of MB under UV-light irradiation are 0.1432 min^{-1} and 0.0345 min^{-1} with ZnO/C(550N) and ZnO(550A), respectively. The rate of degradation MB with ZnO/C

(550N) as catalyst was 4.15 times faster than that of using ZnO (550A). Moreover, the stability of the ZnO/C(550N) was examined for degradation of MB during a three cycle experiment, which was very important for the ZnO/C(550N) to apply in environmental technology. As shown in Fig. 7, the photocatalytic degradation of MB over the ZnO/C (550N) under UV light irradiation was effective, where the photocatalytic efficiency reduced only by 9% after four cycles, indicated that the good stability of the ZnO/C(550N) photocatalyst. More importantly, we found that ZnO/C(550N) photocatalyst could be easily separated and recovered by sedimentation from the photograph inset of Fig. 7, and would greatly promote their practical application to eliminate the organic pollutants from wastewater.

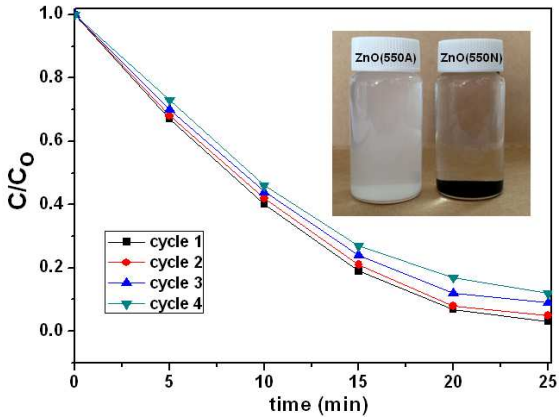

Fig. 7 Four photocatalytic degradation cycles of MB using ZnO/C(550N) nanocomposites under UV light irradiation.

3.3 Photocatalytic Mechanism

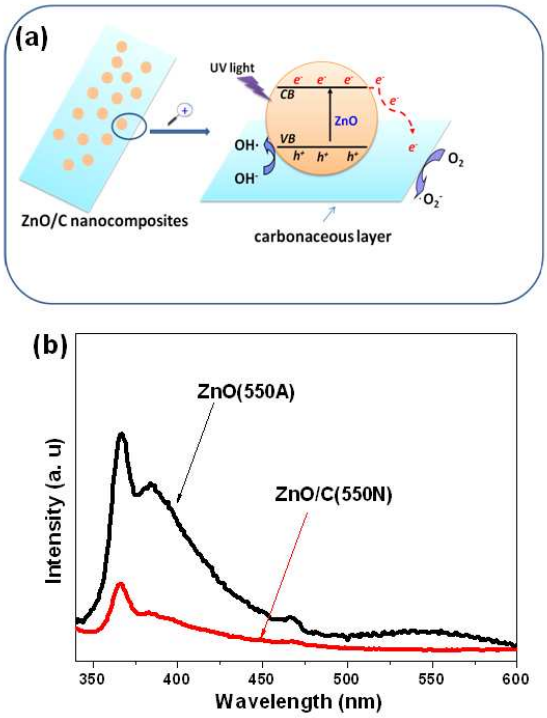

Fig. 8 (a) Proposed mechanisms for the photocatalysis of the ZnO/C (550N) composites. (b) PL emission spectra of ZnO(550A) and ZnO/C(550N).

On the basis of the above results, a proposed mechanism was being discussed to explain the enhancement of the photocatalytic property of the ZnO/C(550N) nanocomposites, as shown in Fig. 8 (a). With UV light irradiation, electrons (e^-) in the valence band of ZnO were excited to the conduction band with the simultaneous generation of holes (h^+) in the valence band, photogenerated electrons (e^-) in ZnO may move freely toward the surface of the carbonaceous layers and excess of valence band holes (h^+) were left in the ZnO to migrate to the surface and reacted with H_2O or OH^- to produce active species such as $OH\cdot$,[40, 41] suggesting that the photogenerated electrons and holes were efficiently separated and the lifetime of the excited electrons and holes could be prolonged in the transfer process, inducing higher quantum efficiency, and thus the photocatalytic activity of ZnO/C(550N) was enhanced greatly. Furthermore, the separation of photogenerated electrons and holes in the

ZnO/C(550N) was confirmed by PL emission spectra of ZnO(550A) and ZnO/C(550N) in Fig. 8 (b). As can be seen, ZnO/C(550N) exhibited much lower emission intensity than that of ZnO (550A),[25, 42, 43] indicating that the recombination of the photogenerated charge carrier was inhibited greatly in the ZnO/C(550N). The efficient charge separation could increase the lifetime of the charge carriers and enhance the efficiency of the interfacial charge transfer to adsorbed substrates, accounting for the higher activity of the ZnO/C(550N) nanocomposites.

4 Conclusions

In summary, ZnO/C nanocomposites were successfully synthesized via one-step calcination method with zinc citrate dihydrate as precursor. The ZnO nanoparticles sized 5-10 nm were evenly and densely distributed over the surface of carbonaceous layers. The synergetic effects between small ZnO nanoparticles and carbonaceous layers make the resultant photocatalyst exhibit excellent photocatalytic activity towards to methylene blue (MB) degradation compared to the ZnO sample which was calcinated in air atmosphere. Furthermore, the ZnO/C(550N) nanocomposites could be easily recycled without obvious decrease of the photocatalytic activity. The simple preparation route, low cost and high photocatalytic activity of the sample will greatly promote its practical application to eliminate the organic pollutants from wastewater.

Acknowledgements

The authors are grateful to the financial supports of National Natural Science Foundation of China (Grant No. 21376051, 21306023, 21106017, and 51077013), Natural Science Foundation of Jiangsu (Grant No. BK20131288), Fund Project for Transformation of Scientific and Technological Achievements of Jiangsu Province of China (Grant No. BA2011086), Specialized

Research Fund for the Doctoral Program of Higher Education of China (Grant No.20100092120047), Key Program for the Scientific Research Guiding Found of Basic Scientific Research Operation Expenditure of Southeast University (Grant No. 3207043101) and Instrumental Analysis Fund of Southeast University.

References

1. M. R. Hoffmann, S. T. Martin, W. Y. Choi and D. W. Bahnemann, *Chem. Rev.*, 1995, **95**, 69-96.

2. B. C. Qiu, M. Y. Xing and J. L. Zhang, *J. Am. Chem. Soc.*, 2014, **136**, 5852-5855.

3. H. J. Wang, F. Q. Sun, Y. Zhang, K. Y. Gu, W. Chen and W. S. Li, *J. Mater. Chem.*, 2011, **21**, 12407-12413.

4. B. Weng, M. Q. Yang, N. Zhang and Y. J. Xu, *J. Mater. Chem. A*, 2014, **2**, 9380-9389.

5. A. B. Djurisic, X. Y. Chen, Y. H. Leung and A. M. C. Ng, *J. Mater. Chem.*, 2012, **22**, 6526-6535.

6. F. Xu, Y. T. Shen, L. T. Sun, H. B. Zeng and Y. N. Lu, *Nanoscale*, 2011, **3**, 5020-5025.

7. G. Williams and P. V. Kamat, *Langmuir*, 2009, **25**, 13869-13873.

8. X. Q. Qiu, L. P. Li, J. Zheng, J. J. Liu, X. F. Sun and G. S. Li, *J. Phys. Chem. C*, 2008, **112**, 12242-12248.

9. X. Q. Qiu, G. S. Li, X. F. Sun, L. P. Li and X. Z. Fu, *Nanotechnology*, 2008, **19**, 215703.

10. J. Bandara, K. Tennakone and P. P. B. Jayatilaka, *Chemosphere*, 2002, **49**, 439-445.

11. Z. C. Wu, C. R. Xu, Y. Q. Wu, H. Yu, Y. Tao, H. Wan and F. Gao, *Crystengcomm*, 2013, **15**, 5994-6002.

12. M. L. Zhang, T. C. An, X. H. Hu, C. Wang, G. Y. Sheng and J. M. Fu, *Appl. Catal. a-Gen.*, 2004, **260**, 215-222.

13. Z. B. Yu, Y. P. Xie, G. Liu, G. Q. Lu, X. L. Ma and H. M. Cheng, *J. Mater. Chem. A*, 2013, **1**, 2773-2776.

14. S. S. Ma, J. J. Xue, Y. M. Zhou and Z. W. Zhang, *J. Mater. Chem. A*, 2014, **2**, 7272-7280.

15. J. B. Mu, C. L. Shao, Z. C. Guo, Z. Y. Zhang, M. Y. Zhang, P. Zhang, B. Chen and Y. C. Liu, *Acs Appl. Mater. Inter.*, 2011, **3**, 590-596.

16. C. Han, M. Q. Yang, B. Weng and Y. J. Xu, *Phys. Chem. Chem. Phys.*, 2014, **16**, 16891-16903.

17. S. S. Ma, J. J. Xue, Y. M. Zhou, Z. W. Zhang and X. Wu, *Crystengcomm*, 2014, **16**, 4478-4484.

18. S. Cho, J. W. Jang, J. S. Lee and K. H. Lee, *Crystengcomm*, 2010, **12**, 3929-3935.

19. Y. Guo, H. S. Wang, C. L. He, L. J. Qiu and X. B. Cao, *Langmuir*, 2009, **25**, 4678-4684.

20. L. W. Zhang, H. Y. Cheng, R. L. Zong and Y. F. Zhu, *J. Phys. Chem. C*, 2009, **113**, 2368-2374.

21. T. G. Xu, L. W. Zhang, H. Y. Cheng and Y. F. Zhu, Appl. Catal. B-Environ., 2011, 101, 382-387.

22. H. B. Fu, T. G. Xu, S. B. Zhu and Y. F. Zhu, *Environ. Sci. Technol.*, 2008, **42**, 8064-8069.

23. P. V. Kamat, *J. Phys. Chem. Lett.*, 2010, **1**, 520-527.

24. A. Dev, S. K. Panda, S. Kar, S. Chakrabarti and S. Chaudhuri, *J. Phys. Chem. B*, 2006, **110**, 14266-14272.

25. R. X. Zhang, L. Z. Fan, Y. P. Fang and S. H. Yang, *J. Mater. Chem.*, 2008, **18**, 4964-4970.

26. Z. H. Ni, Y. Y. Wang, T. Yu and Z. X. Shen, *Nano Res.*, 2008, **1**, 273-291.

27. C. Chen, W. M. Cai, M. C. Long, B. X. Zhou, Y. H. Wu, D. Y. Wu and Y. J. Feng, *Acs Nano*,

2010, **4**, 6425-6432.

28. D. Graf, F. Molitor, K. Ensslin, C. Stampfer, A. Jungen, C. Hierold and L. Wirtz, *Nano Lett.*, 2007, **7**, 238-242.

29. L. C. Sim, K. H. Leong, S. Ibrahim and P. Saravanan, *J. Mater. Chem. A*, 2014, **2**, 5315-5322.

30. M. C. Long, Y. L. Qin, C. Chen, X. Y. Guo, B. H. Tan and W. M. Cai, *J. Phys. Chem. C*, 2013, **117**, 16734-16741.

31. C. H. Wu, Y. Z. Zhang, S. Li, H. J. Zheng, H. Wang, J. B. Liu, K. W. Li and H. Yan, *Chem. Eng. J.*, 2011, **178**, 468-474.

32. L. Q. Jiang and L. Gao, *Mater. Chem. Phys.*, 2005, **91**, 313-316.

33. K. S. W. Sing, D. H. Everett, R. A. W. Haul, L. Moscou, R. A. Pierotti, J. Rouquerol and T. Siemieniewska, *Pure Appl. Chem.*, 1985, **57**, 603-619.

34. D. D. Lin, H. Wu, R. Zhang and W. Pan, *Chem. Mater.*, 2009, **21**, 3479-3484.

35. P. F. Ji, J. L. Zhang, F. Chen and M. Anpo, *Appl. Catal. B-Environ.*, 2009, **85**, 148-154.

36. Y. C. Hsu, H. C. Lin, C. W. Lue, Y. T. Liao and C. M. Yang, *Appl. Catal. B-Environ.*, 2009, **89**, 309-314.

37. H. S. Teng and C. T. Hsieh, *Ind. Eng. Chem. Res.*, 1998, **37**, 3618-3624.

38. S. S. Ma, R. Li, C. P. Lv, W. Xu and X. L. Gou, *J. Hazard. Mater.*, 2011, **192**, 730-740.

39. L. Y. Yang, S. Y. Dong, J. H. Sun, J. L. Feng, Q. H. Wu and S. P. Sun, *J. Hazard. Mater.*, 2010, **179**, 438-443.

40. S. Liu, E. Y. Guo and L. W. Yin, *J. Mater. Chem.*, 2012, **22**, 5031-5041.

41. M. Y. Xing, X. Li and J. L. Zhang, *Sci. Rep-Uk*, 2014, **4**.

42. M. Samadi, H. A. Shivaee, A. Pourjavadi and A. Z. Moshfegh, *Appl. Catal. a-Gen.*, 2013, **466**,

153-160.

43. H. B. Zeng, G. T. Duan, Y. Li, S. K. Yang, X. X. Xu and W. P. Cai, *Adv. Funct. Mater.*, 2010, **20**, 561-572.